

29 Mar 99 draft

# Red and Blue Shifted Broad Lines in Luminous Quasars <sup>1</sup>

D. H. McIntosh<sup>2</sup>, H.-W. Rix<sup>3</sup>, M. J. Rieke<sup>2</sup>, C. B. Foltz<sup>4</sup>

## ABSTRACT

We have observed a sample of 22 luminous quasars, in the range  $2.0 \lesssim z \lesssim 2.5$ , at  $1.6\mu\text{m}$  with the near-infrared (NIR) spectrograph FSPEC on the Multiple Mirror Telescope. Our sample contains 13 radio-loud and 9 radio-quiet objects. We have measured the systemic redshifts  $z_{\text{sys}}$  directly from the strong [O III] $\lambda 5007$  line emitted from the narrow-line-region. From the same spectra, we have found that the non-resonance broad H $\beta$  lines have a systematic mean *redward* shift of  $520 \pm 80 \text{ km s}^{-1}$  with respect to systemic. Such a shift was *not* found in our identical analysis of the low-redshift sample of Boroson & Green. The amplitude of this redshift is comparable to half the expected gravitational redshift and transverse Doppler effects, and is consistent with a correlation between redshift differences and quasar luminosity. From data in the literature, we confirm that the high-ionization rest-frame ultraviolet broad lines are *blueshifted*  $\sim 550\text{--}1050 \text{ km s}^{-1}$  from systemic, and that these velocity shifts systematically increase with ionization potential. Our results allow us to quantify the known bias in estimating the ionizing flux from the inter-galactic-medium  $J_{\nu}^{\text{IGM}}$  via the Proximity Effect. Using redshift measurements commonly determined from strong broad line species, like Ly $\alpha$  or C IV $\lambda 1549$ , results in an over-estimation of  $J_{\nu}^{\text{IGM}}$  by factors of  $\sim 1.9 - 2.3$ . Similarly, corresponding lower limits on the density of baryons  $\Omega_b$  will be over-estimated by factors of  $\sim 1.4 - 1.5$ . However, the low-ionization Mg II $\lambda 2798$  broad line is within  $\sim 50 \text{ km s}^{-1}$  of systemic, and thus would be the line of choice for determining the true redshift of  $1.0 < z < 2.2$  quasars without NIR spectroscopy, and  $z > 3.1$  objects using NIR spectroscopy.

*Subject headings:* cosmology: miscellaneous — infrared: general — quasars: emission lines — quasars: general — relativity

---

<sup>1</sup>Observations reported here were obtained at the Multiple Mirror Telescope Observatory, a facility operated jointly by the University of Arizona and the Smithsonian Institution.

<sup>2</sup>Steward Observatory, University of Arizona, Tucson, AZ 85721

<sup>3</sup>Max Planck Institut für Astronomie, Heidelberg, Germany

<sup>4</sup>Multiple Mirror Telescope Observatory, University of Arizona, Tucson, AZ 85721

## 1. Introduction

Defining the center-of-mass (COM  $\equiv$  systemic) rest-frame, thus  $z_{\text{sys}}$ , of quasars (QSOs) and of their host galaxies is important for a number of reasons. First, it is crucial for estimating the ionizing flux from the inter-galactic-medium  $J_{\nu}^{\text{IGM}}$  via the Proximity Effect (Bajtlik, Duncan & Ostriker 1988). To estimate the redshift range ( $z_{\text{sys}} - z_{\text{Ly}\alpha}$ ) over which Ly $\alpha$  absorbers are underpopulated, we need to know  $z_{\text{sys}}$  accurately. An error of 1000 km s $^{-1}$  in  $z_{\text{sys}}$  leads to a factor of  $\sim 2.6$  difference in the inferred  $J_{\nu}^{\text{IGM}}$  (Espey 1993). In turn, precise estimates of  $J_{\nu}^{\text{IGM}}$  are needed to understand the ionization balance of the IGM and the structure of the Ly $\alpha$  Forest. Furthermore, accurate knowledge of the systemic frame is important to understanding the ‘central engine’ and the broad-line-region (BLR) physics. Inflow, outflow and radiative transfer effects may lead to offsets between the emission line centroids and  $z_{\text{sys}}$ . The value of  $z_{\text{sys}}$  also plays a critical role in understanding the kinematics of ‘associated’ ( $z_{\text{abs}} \approx z_{\text{em}}$ ) absorption line systems (Foltz *et al.* 1986) and the nature of the ‘ $z_{\text{abs}} > z_{\text{em}}$ ’ metal line systems (Gaskell 1982). In both cases, determination of  $z_{\text{sys}}$  is necessary to understand whether the absorbing gas is in- or out-flowing, or at rest with respect to the QSO.

As Tytler & Fan (1992) first showed, the QSO redshift as measured by different broad emission lines systematically depends on ionization potential. In general, it has been well documented (Gaskell 1982; Espey *et al.* 1989; Brotherton *et al.* 1994; and references therein) that broad emission lines from highly ionized species (HILs; *e.g.* C IV $\lambda$ 1549, C III] $\lambda$ 1909, N V $\lambda$ 1240), as well as Ly $\alpha$ , are systematically blueshifted 500–1500 km s $^{-1}$  with respect to broad emission lines from lower ionization species (LILs; *e.g.* Mg II $\lambda$ 2798, O I $\lambda$ 1305), and the permitted H I Balmer series. In contrast, redshifts from narrow emission lines (*e.g.* [O III] $\lambda$ 5007) in low redshift ( $z < 1$ ) QSOs and Seyfert galaxies are observed to be within 100 km s $^{-1}$  of the broad Mg II and Balmer lines (Gaskell 1982; Tytler & Fan 1992; Boroson & Green 1992; Laor *et al.* 1995; and Corbin & Boroson 1996). Furthermore, in local AGN, redshifts from narrow forbidden lines have shown agreement to  $\lesssim 100$  km s $^{-1}$  of the accepted systemic frame determined by stellar absorption features and H I 21 cm emission in the host galaxies (Gaskell 1982; Vrtilek & Carleton 1985, Hutchings, Gower & Price 1987), and are within  $\pm 200$  km s $^{-1}$  of the CO emission (Alloin *et al.* 1992). Since the narrow emission originates from a large volume of gas centered on the QSO (*i.e.* the narrow-line-region with  $r_{\text{NLR}} \sim 1$  kpc), Penston (1977) first proposed that it is likely that the narrow forbidden lines give the COM redshift.

At higher redshifts ( $z > 1.5$ ) the strong narrow lines can only be detected in the NIR. Early NIR spectroscopy of a single bright  $z = 2.09$  QSO showed H $\alpha$ , H $\beta$  and narrow [O III] emission had similar redshifts to the LILs, supporting the low redshift studies that claimed Balmer lines provided a reliable measure of  $z_{\text{sys}}$  (Carswell *et al.* 1991). However, Nishihara *et al.* (1997) took NIR spectra of four  $z > 1.5$  QSOs and found the broad H $\alpha$  line to be redshifted on average by  $430 \pm 170$  km s $^{-1}$  from the systemic [O III] narrow line.

From our total sample of 32 bright ( $V \leq 18.0$  mag),  $2.0 \lesssim z \lesssim 2.5$  QSOs with NIR  $H$ -band

spectra (see McIntosh, Rieke, Rix, Foltz & Weymann 1999; hereafter M99), we selected the set of 22 objects with detected  $[\text{O III}]\lambda 5007$  emission ( $[\text{O III}] \text{EW} \geq 5\text{\AA}$ , except Q0842+345, Q1011+091, and Q1158-187 for which the low S/N prohibited reliable line identification). This nearly unprecedented detection of strong emission lines from the NLR of distant, high luminosity QSOs has provided the direct measurement of  $z_{\text{sys}}$  via the rest-frame  $[\text{O III}]\lambda 5007$  line center. Consequently, this unique data set allows direct comparisons between the COM frame and a variety of resonance and recombination broad line centers in this sample. In addition, each spectrum contains the broad  $\text{H}\beta$  line, thus, we are able to directly compare the NLR redshift with a redshift obtained from BLR emission in the same spectrum.

## 2. Emission Line Redshift Measurements

To measure  $z_{\text{sys}}$  for each QSO, we fit roughly the upper half of the  $[\text{O III}]\lambda 5007$  line with a Gaussian, except for three objects (Q1228+077, Q1331+170 and Q1416+091) for which the peak or centroid of the  $[\text{O III}]$  line was used due to the poor S/N of these spectra. This fitting procedure provided line center measurements with much smaller uncertainties compared with the broad  $\text{H}\beta$  measurements (see below). We estimated the uncertainties to be  $\sigma \sim \pm 50 \text{ km s}^{-1}$ . The measured systemic redshifts are presented in column (2) of Table 1.

To determine the QSO broad  $\text{H}\beta$  redshift  $z_{\text{em}}$ , we shifted each spectrum to its systemic frame and fit it with a set of templates representing  $[\text{O III}]$ ,  $\text{H}\beta$ ,  $\text{Fe II}$  and continuum emission features using a  $\chi^2$  optimization routine (as described in M99). All components except  $\text{H}\beta$  were subtracted from the data spectrum resulting in an  $\text{H}\beta$  line spectrum. The central wavelength of the broad component was obtained by fitting a single Gaussian to all portions of the line profile with relative flux  $\leq \frac{3}{4}$  of the maximum (see M99). The broad  $\text{H}\beta$  line centers measured in the systemic frame, with their  $\pm 1\sigma$  uncertainties, are given in column (3) of Table 1. In addition, the emission redshifts derived from broad  $\text{H}\beta$  are listed in column (4).

Table 1. Observed Redshift Parameters

QSO	$z_{\text{sys}}$	Broad H $\beta$		
		$\lambda_{\text{ctr}}$ (Å)	$z_{\text{em}}$	$\Delta v$ (km s $^{-1}$ )
BAL0043+008	2.146	4866 ± 2	2.149	310 ± 120
Q0049+014	2.307	4862 ± 4	2.308	60 ± 310
Q0109+022	2.351	4868 ± 6	2.356	430 ± 370
Q0123+257	2.370	4868 ± 3	2.375	430 ± 190
Q0153+744	2.341	4871 ± 2	2.348	620 ± 190
Q0226-038	2.073	4858 ± 5	2.071	-190 ± 310
Q0421+019	2.056	4873 ± 3	2.064	740 ± 190
Q0424-131	2.168	4866 ± 3	2.171	310 ± 190
Q0552+398	2.363	4867 ± 3	2.367	370 ± 190
HE1104-181	2.318	4870 ± 3	2.324	560 ± 190
Q1148-001	1.980 <sup>a</sup>	...	...	...
Q1222+228	2.058	4858 ± 3	2.056	-190 ± 190
Q1228+077	2.389	4860 ± 3	2.388	-60 ± 190
PG1247+267	2.042	4873 ± 1	2.050	740 ± 60
Q1331+170	2.097	4861 ± 4	2.097	0 ± 250
Q1416+091	2.017	4851 ± 8	2.011	-620 ± 490
Q1435+638	2.066	4875 ± 4	2.075	860 ± 250
Q1448-232	2.220	4876 ± 2	2.230	930 ± 120
Q1704+710	2.010	4879 ± 5	2.021	1110 ± 310
BAL2212-179	2.228	4864 ± 5	2.230	190 ± 310
Q2251+244	2.359	4852 ± 4	2.353	-560 ± 250
Q2310+385	2.181	4869 ± 4	2.186	490 ± 250

<sup>a</sup>Redshift of this QSO is such that H $\beta$  line center is blueward of  $H$ -band window.

### 3. Velocity Shifts

Comparing the  $z_{\text{sys}}$  and the broad  $\text{H}\beta$   $z_{\text{em}}$  measurements for each QSO (see Table 1) reveals a velocity shift  $\Delta v$  relative to the systemic frame. A  $\Delta v > 0$  corresponds to a redward shift of  $\text{H}\beta$  with respect to systemic, while a negative  $\Delta v$  represents a blueshift. The velocity shifts for broad  $\text{H}\beta$  are tabulated in column (5) of Table 1, where the uncertainties are determined by the broad  $\text{H}\beta$  component.

This is the first sizeable sample of high luminosity QSOs to permit a statistical comparison of the velocity shifts of various UV rest-frame broad line redshifts relative to *systemic*. Therefore, we compiled the published redshifts for each object in Table 2, and calculated  $\Delta v$  for each line species:

$$\Delta v = \left( \frac{z_{\text{line}} - z_{\text{sys}}}{1 + z_{\text{sys}}} \right) c, \quad (1)$$

where  $z_{\text{line}}$  is the published redshift. The distribution of velocity shifts for each UV line species is plotted separately in Figure 1. All blueshifts larger than  $2250 \text{ km s}^{-1}$  are due to a single radio-loud object (Q2251+244) with strong [O III] emission (see M99, Fig. 1). The  $z_{\text{sys}}$  measurements are accurate to  $\sim 50 \text{ km s}^{-1}$  on average, while the majority of the published redshifts are known to  $\pm 0.001$  which corresponds to roughly  $\pm 100 \text{ km s}^{-1}$ .

Table 2. Published Emission Line Redshifts

QSO	Ly $\alpha$ $\lambda 1216$	Refs. <sup>a</sup>	N V $\lambda 1240$	Refs. <sup>a</sup>	Si IV/O IV] <sup>b</sup> $\lambda 1400$	Refs. <sup>a</sup>	C IV $\lambda 1549$	Refs. <sup>a</sup>	C III] $\lambda 1909$	Refs. <sup>a</sup>	Mg II $\lambda 2798$	Refs. <sup>a</sup>
BAL0043+008	...	...	...	...	...	...	2.141	1,2	2.143	2,3	2.143	3 <sup>c</sup>
Q0049+014	2.31	4	...	...	...	...	2.285	5	2.30	6 <sup>d</sup>	...	...
Q0109+022	2.35	4	...	...	...	...	2.348	5	2.34	6 <sup>d</sup>	...	...
Q0123+257	2.360	7,8 <sup>d</sup>	...	...	...	...	2.356	7,8 <sup>d</sup>	2.36	6 <sup>d</sup>	...	...
Q0153+744	2.342	9	2.340	9	2.340	9	2.339	9	2.339	9	2.349	9
Q0226-038	2.069	10-12	2.058	12	2.057	10,12,13	2.064	10-14	2.064	14	2.073	14
Q0421+019	2.048	12,15	...	...	...	...	2.051	15	2.053	12,14	2.056	14
Q0424-131	2.160	13,16	...	...	2.168	13	2.164	13,14,16	2.164	14,16	2.166	14,16
Q0552+398	2.362	4,17	...	...	...	...	...	...	...	...	...	...
HE1104-181	2.315	18	...	...	...	...	2.312	18-20	...	...	...	...
Q1148-001	1.979	11,12	...	...	1.975	10,11,12	1.979	10-14,21	1.979	10,14,21	1.978	14,21
Q1222+228	2.046	11,12,16	2.049	12	2.046	12,13	2.042	11-13,16	2.053	16	2.056	16
Q1228+077	2.388	4,22,23	...	...	...	...	2.389	24	2.392	12	...	...
PG1247+267	2.040	11-13	2.042	12	2.040	12,13	2.039	11-13	2.043	25 <sup>d</sup>	...	...
Q1331+170	2.084	11,12,16,26	2.079	12,26	2.086	12,13	2.079	11-13,16,26	2.086	16,26	2.095	16,26
Q1416+091	...	...	...	...	...	...	...	...	2.012	14	2.018	14
Q1435+638	...	...	...	...	2.072	13	2.066	13,14	2.062	14,27	2.061	14
Q1448-232	2.216	16,28	...	...	...	...	2.216	16,28,29	2.214	16,29	2.223	16
Q1704+710	...	...	...	...	...	...	...	...	2.011	14	2.019	14
BAL2212-179	2.220	30 <sup>e</sup>	2.205	30 <sup>e</sup>	2.218	30 <sup>e</sup>	2.209	30 <sup>e</sup>	...	...	...	...
Q2251+244	2.330	7,10,31	...	...	2.328	10,12	2.323	7,10,12,31	2.318	12,31	...	...
Q2310+385	...	...	...	...	...	...	2.175	32	...	...	...	...

<sup>a</sup>Multiple references indicate that the redshift is an average.

<sup>b</sup> $\lambda 1400$  blend of the Si IV doublet and the O IV multiplet.

<sup>c</sup>Redshift extrapolated from an emission line profile comparison.

<sup>d</sup>Redshift measured directly from published spectrum.

<sup>e</sup>Redshift measured directly from digital spectrum.

References. — (1) Osmer *et al.* 1994; (2) Turnshek *et al.* 1980; (3) Hartig & Baldwin 1986; (4) Wolfe *et al.* 1986; (5) Schneider *et al.* 1994; (6) Pei *et al.* 1991; (7) Schmidt 1975; (8) Barlow & Sargent 1997; (9) Lawrence *et al.* 1996; (10) Gaskell 1982; (11) Young *et al.* 1982; (12) Tytler & Fan 1992; (13) Sargent *et al.* 1988; (14) Steidel & Sargent 1991; (15) Schmidt 1977; (16) Espey *et al.* 1989; (17) Wills & Wills 1976; (18) Smette *et al.* 1995; (19) Wisotzki *et al.* 1993; (20) Reimers *et al.* 1996; (21) Aldcroft *et al.* 1994; (22) Vaucher & Weedman 1980; (23) Robertson & Shaver 1983; (24) Sramek & Weedman 1978; (25) Green *et al.* 1980; (26) Carswell *et al.* 1991; (27) Laor *et al.* 1995; (28) Jian-sheng *et al.* 1984; (29) Ulrich 1989; (30) Morris *et al.* 1991; (31) Barthel *et al.* 1990; (32) B. J. Wills 1997, private communication

#### 4. Results and Discussion

From the above analysis, we find:

1. that the  $\text{H}\beta$  broad component emission has a weighted mean redshift of  $520 \pm 80 \text{ km s}^{-1}$  relative to  $z_{\text{sys}}$ , with a sample variance of  $360 \text{ km s}^{-1}$ .
2. that on average the  $\text{Mg II}\lambda 2798$  based redshift is within  $\sim 50 \text{ km s}^{-1}$  of systemic, confirming that LILs should provide reliable  $z_{\text{sys}}$  estimates (Carswell *et al.* 1991). The rest wavelength and strength of Mg II emission make it the line of choice for determining  $z_{\text{sys}}$  of distant ( $1.0 < z < 2.2$ ) QSOs without NIR spectroscopy, or even more remote ( $z \gtrsim 3.1$ ) objects using NIR spectroscopy.
3. confirmation of the following effects: (i) The average blueshift ( $\sim 600 - 1100 \text{ km s}^{-1}$ ) of the HILs relative to the LIL Mg II. (ii) The correlation between average blueward velocity shift and ionization potential for each resonance broad line species.
4. no correlation between QSO radio type (*i.e.* radio-loud versus radio-quiet) and any of the line species velocity shifts.

##### 4.1. Redshifted Balmer Lines

The mean redshift of broad  $\text{H}\beta$  is similar to that found for  $\text{H}\alpha$  in a small sample (4) of luminous  $z \sim 2$  QSOs (Nishihara *et al.* 1997). Yet at lower redshifts ( $z < 1$ ), Balmer emission gives the same redshift to within  $100 \text{ km s}^{-1}$  of narrow forbidden emission. Given that  $z \sim 2$  QSOs are more luminous than their present-day counterparts, perhaps this observed trend of increased Balmer redshift with increased  $z_{\text{sys}}$  represents a luminosity dependence. In fact, we find a correlation between  $\text{H}\beta$  redshift and QSO rest-frame  $V$ -band luminosity (from M99), such that the  $\sim 100$  times less luminous sample of Boroson & Green (1992) exhibits a mean broad  $\text{H}\beta$  redshift of  $< 100 \text{ km s}^{-1}$  (see Figure 2). We conclude that the use of Balmer emission lines to measure  $z_{\text{sys}}$  may not be prudent for more distant, and thus more luminous QSOs.

The magnitude of the redward Balmer shift may be partially due to relativistic effects (Netzer 1977). Recent studies (*e.g.* Corbin & Boroson 1996) have suggested a connection between the luminosity dependence of QSO broad line redward asymmetries and gravitational redshifts due to virialized motions near super-massive ( $\sim 10^9 - 10^{10} M_{\odot}$ ) black holes. Assuming BLR emission from a gravitationally bound (virialized), spherical ensemble of clouds at  $r \sim 0.1 \text{ pc}$  allows the conversion from the observed mean broad line width to the mean line-of-sight (LOS) velocity and the true average cloud velocity:  $\langle v_{\text{FWHM}} \rangle = 2\langle v_{\text{LOS}} \rangle = \frac{2}{\sqrt{3}}\langle v_{\text{cloud}} \rangle$ . We measured the weighted mean line width  $\langle v_{\text{FWHM}} \rangle = 8750 \pm 570 \text{ km s}^{-1}$ , with a sample variance of  $2550 \text{ km s}^{-1}$ , from the  $\text{H}\beta$  broad component fitting (M99). The gravitational redshifting of emission from clouds deep

within the potential well of the super-massive black hole is  $\Delta v_{\text{GR}} \simeq \frac{\langle v_{\text{cloud}}^2 \rangle}{c} \simeq 190 \pm 20 \text{ km s}^{-1}$ . In addition, emission from clouds moving perpendicular to our LOS experiences a transverse Doppler shift of  $\Delta v_{\text{TDS}} \simeq \frac{v_1^2}{2c} \simeq \frac{\langle v_{\text{cloud}}^2 \rangle}{3c} \simeq 60 \pm 10 \text{ km s}^{-1}$ .

The combination of these two relativistic effects can account for roughly half of the  $520 \pm 80 \text{ km s}^{-1}$  Balmer redshift. Although intriguing, it is unclear why this emission would not also exhibit Doppler beaming effects (*e.g.* Laor 1991) and why the HILs, which reverberation mapping studies have placed at the same distance, have blueshifts.

#### 4.2. Cosmological Implications of the $z_{\text{sys}}$ Measurements

HILs, like Ly $\alpha$  or C IV, are not directly measuring  $z_{\text{sys}}$ . Specifically, for this sample we find Ly $\alpha$  and C IV to be blueshifted on average  $550$  and  $860 \text{ km s}^{-1}$ , respectively, relative to systemic. Therefore, using redshifts acquired from these lines will result in the over-estimation of  $J_{\nu}^{\text{IGM}}$  via Proximity Effect calculations by respective factors of roughly  $1.9$  and  $2.3$  (Espey 1993). In addition, the lower limit to the density of baryonic matter in the Universe  $\Omega_b$ , is proportional to the square root of  $J_{\nu}^{\text{IGM}}$  (Rauch *et al.* 1997). Therefore, over-estimating the strength of the background flux translates into an over-estimation of the lower limit of  $\Omega_b$  by factors of about  $1.4$  and  $1.5$ .

We are grateful to Ray Weymann who generously reviewed this Letter and provided insightful comments and suggestions. We acknowledge helpful discussions with Robert Antonucci, Jill Bechtold, John Cocke, Mike Corbin, Rolf Kudritzki, Phil Pinto, Jennifer Scott, Matthias Steinmetz and Belinda Wilkes. And we thank the anonymous referee for fair and thoughtful suggestions that improved our Letter. This research was supported, in part, by National Science Foundation Grants AST 9529190 and 9803072.

## REFERENCES

Aldcroft, T. L., Bechtold, J., & Elvis, M. 1994, ApJS, 93, 1

Alloin, D., Barvainis, R., Gordon, M. A., & Antonucci, R. R. J. 1992, A&A, 265, 429

Bajtlik, S., Duncan, R. C., & Ostriker, J. P. 1988, ApJ, 327, 570

Barlow, T. A., Sargent, W. L. W. 1997, AJ, 113, 136

Barthel, P. D., Tytler, D., & Thomson, B. 1990, A&AS, 82, 339

Boroson, T. A., & Green, R. F. 1992, ApJS, 80, 109

Brotherton, M. S., Wills, B. J., Steidel, C. C., & Sargent, W. L. W. 1994a, ApJ, 423, 131

Carswell, R. F. *et al.* 1991, ApJ, 381, L5

Corbin, M. R., & Boroson, T. A. 1996, ApJS, 107, 69

Espey, B. R., Carswell, R. F., Bailey, J. A., Smith, M. G., & Ward, M. J. 1989, ApJ, 342, 666

Espey, B. R. 1993, ApJ, 411, L59

Foltz, C. B., Weymann, R. J., Peterson, B. M., Sun, L., Malkan, M. A., & Chaffee, F. H. 1986, ApJ, 307, 504

Gaskell, C. M. 1982, ApJ, 263, 79

Green, R. F. *et al.* 1980, ApJ, 239, 483

Hartig, G. F., & Baldwin, J. A. 1986, ApJ, 302, 64

Hutchings, J. B., Gower, A. C., & Price, R. 1987, AJ, 93, 6

Jian-sheng, C., Morton, D. C., Peterson, B. A., Wright, A. E., & Jauncey, D. L. 1984, *Proceedings of the Astronomical Society of Australia*, vol. 5, p. 355

Laor, A. 1991, ApJ, 376, 90

Laor, A., Bahcall, J. N., Jannuzi, B. T., Schneider, D. P., & Green, R. F. 1995, ApJS, 99, 1

Lawrence, C. L., Zucker, J. R., Readhead, A. C. S., Unwin, S. C., Pearson, T. J., & Xu, W. 1996, ApJS, 107, 541

McIntosh, D. H., Rieke, M. J., Rix, H.-W., Foltz, C. B., & Weymann, R. J. 1999, ApJ, 514, in press (M99)

Morris, S. L., Weymann, R. J., Anderson, S. F., Hewett, P. C., Francis, P. J., Foltz, C. B., Chaffee, F. H., & MacAlpine, G. M. 1991, AJ, 102, 1627

Netzer, H. 1977, MNRAS, 181, 89P

Nishihara, E., Yamashita, T., Yoshida, M., Watanabe, E., Okumura, S.-I., Mori, A., & Iye, M. 1997, ApJ, 488, L27

Osmers, P. S., Porter, A. C., & Green, R. F. 1994, ApJ, 436, 678

Pei, Y. C., Fall, S. M., & Bechtold, J. 1991, ApJ, 378, 6

Penston, M. V. 1977, MNRAS, 180, 27P

Rauch, M. *et al.* 1997, ApJ, 489, 7

Reimers, D., Köhler, T., & Wisotzki, L. 1996, A&AS, 115, 235

Robertson, J. G., & Shaver, P. A. 1983, MNRAS, 204, 69

Sargent, W. L. W., Boksenberg, A., & Steidel, C. C. 1988, ApJS, 68, 539

Schmidt, M. 1975, ApJ, 195, 253

Schmidt, M. 1977, ApJ, 217, 358

Schneider, D. P., Schmidt, M., & Gunn, J. E. 1994, AJ, 107, 1245

Smette, A., Robertson, J. G., Shaver, P. A., Reimers, D., Wisotzki, L., & Köhler, T. 1995, A&AS, 113, 199

Sramek, R. A., & Weedman, D. W. 1978, ApJ, 221, 468

Steidel, C. S., & Sargent, W. L. W. 1991, ApJ, 382, 433

Turnshek, D. A., Weymann, R. J., Liebert, J. W., Williams, R. E., Strittmatter, P. A. 1980, ApJ, 238, 488

Tytler, D., & Fan, X.-M. 1992, ApJS, 79, 1

Ulrich, M.-H. 1989, A&A, 220, 71

Vaucher, R. G., & Weedman, D. W. 1980, ApJ, 240, 10

Vrtilek, J. M., & Carleton, N. P. 1985, ApJ, 294, 106

Wills, D., & Wills, B. J. 1976, ApJS, 31, 143

Wisotzki, L., Köhler, T., Kayser, R., & Reimers, D. 1993, A&A, 278, L15

Wolfe, A. M., Turnshek, D. A., Smith, H. E., & Cohen, R. D. 1986, ApJS, 61, 249

Young, P., Sargent, W. L. W., & Boksenberg, A. 1982, ApJS, 48, 455

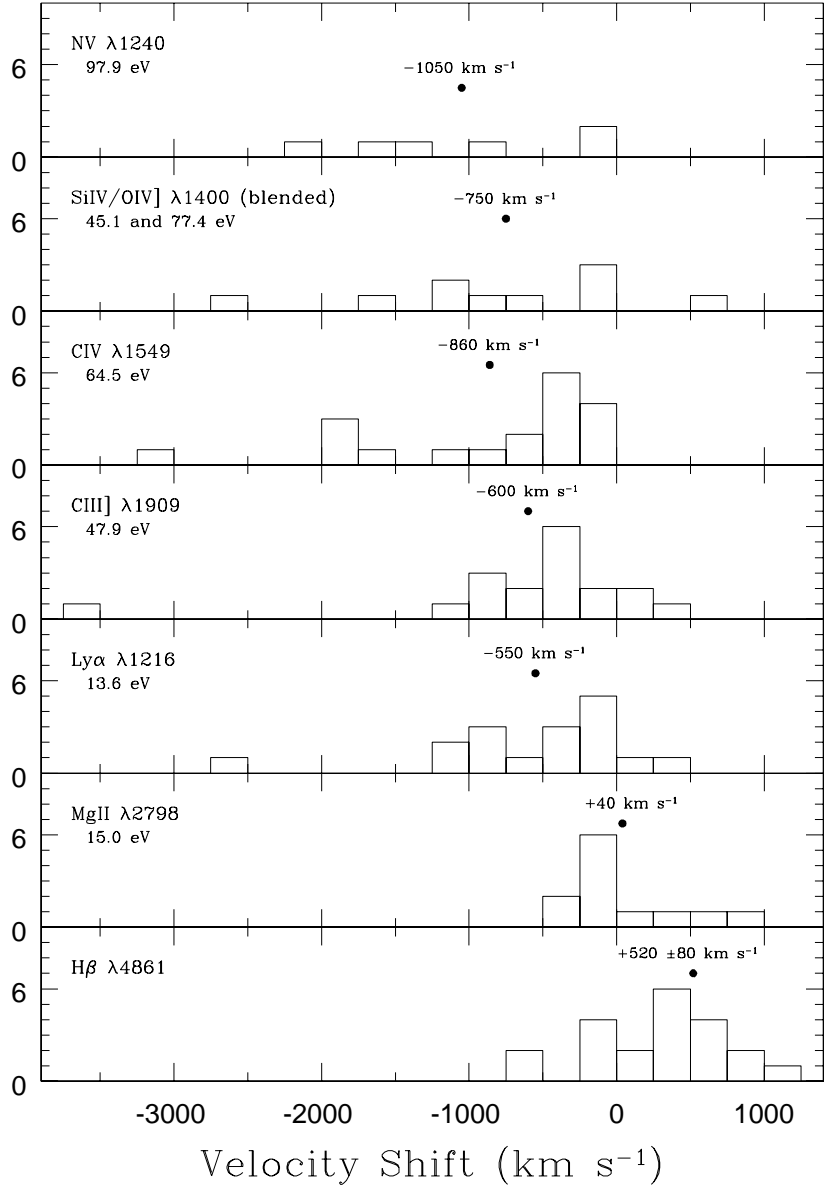


Fig. 1.— Distributions of the broad emission line velocity shifts relative to the systemic frame (given by the [O III] $\lambda 5007$  emission line center). A negative velocity shift corresponds to a blueshift relative to systemic, while a positive shift represents a redshift. The velocity bins are  $\sim 1\langle\sigma\rangle$  for the broad H $\beta$  shifts and  $\sim 2.5\langle\sigma\rangle$  for the UV rest-frame line shifts. The unweighted average of each blueshifted distribution is plotted as a solid dot, while the weighted mean with  $\pm 1\sigma$  uncertainty is shown for the redshifted broad H $\beta$  distribution. The ionization potential  $\chi_{\text{ion}}$  of each UV line is given, as well as its rest wavelength (in  $\text{\AA}$ ).

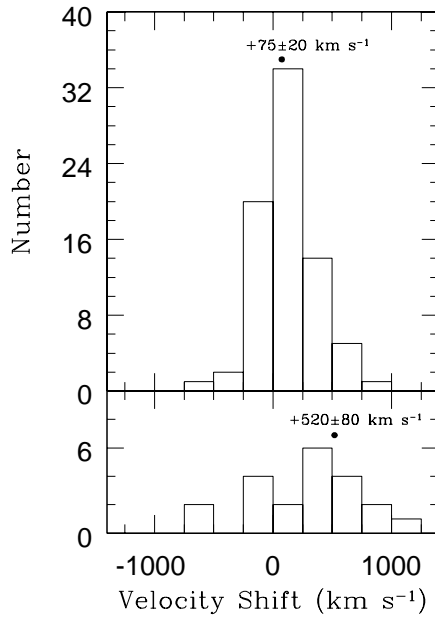


Fig. 2.— The comparison between the distributions of broad H $\beta$  velocity shifts for the nearby ( $z < 0.5$ , upper panel), lower luminosity sample of Boroson & Green (1992); and our  $\sim 100$  times more luminous, high redshift ( $z > 2.0$ , lower panel) sample. The broad component H $\beta$  line centers, used to calculate the velocity shifts for each sample, were measured using the identical procedure (described in §2.2) and [O III] EW  $\geq 5\text{\AA}$  selection criteria. The mean rest-frame V-band luminosities of these two samples differ by roughly a factor of 100 (see M99). The data bin size is  $\sim 1\langle\sigma\rangle$  of the broad H $\beta$  velocity shifts found in the more luminous sample. The mean of each distribution is plotted as a solid dot.